

정전형 마이크로 액츄에이터의 주파수 응답 특성 해석

민동기  
삼성종합기술원 Storage Lab.

Frequency Response Analysis of Electrostatic Microactuators

Dong-Ki Min  
Storage Lab., Samsung Advanced Institute of Technology, P.O.Box 111, Suwon, Korea

**Abstract** - The admittance of one-port electrostatic actuator are modeled using the steady-state sinusoidal response. Also the admittance of the differential type actuator is derived taking the practical conditions into consideration, although it has no admittance in ideal case. It is a function of biasing error, driving error, and capacitive mismatch including parasitic capacitors. The validity of the admittance model is proved by comparing between the modeled and measured admittances. The distortion in the frequency response curve measured by a capacitive sensor is analyzed and it is concluded that the admittance is the main cause of this distortion.

1. Introduction

Admittance of one-port electrostatic actuator or sensor in Fig.1(a) is well understood through equivalent circuit modeling[1][2]. Its frequency response curve shows the mechanical behavior of the actuator and how it couples with the electrical behavior like quartz crystal devices. But, when evaluating a differential type electrostatic actuator in Fig.2(b) with a capacitive sensor, its characteristic like one-port electrostatic actuators or quartz crystal devices can be seen: parallel resonant or anti-resonant frequency.

In this paper, after deriving the admittances of one-port actuator and a differential type actuator from the steady-state sinusoidal response considering the practical conditions, the modeled admittances and the measured admittances are compared. Then the distortion in the frequency response curve obtained by a capacitive sensor of which the demodulator is a sample and hold device is analyzed and the main factor affecting this distortion is given.

2. One-Port Electrostatic Actuator

2.1 Mechanical Model

A mechanical system can be described by a simple lumped parameter model and then its transfer function,  $T_m(s)$ , will be given as

$$T_m(s) = (Ms^2 + Cs + K)^{-1}, \tag{1}$$

where  $M$  is a mass,  $C$  is a damping constant, and  $K$  is a spring constant.

Consider a sinusoidal driving voltage,  $v_d = V_d \sin \omega t$ , with a bias voltage,  $V_s$ . If this voltage is applied as shown in Fig.1(a), then an electrostatic force,  $f$ , will be generated as  $f = (1/2)(\partial c / \partial x)(V_s + v_d)^2$  and it can be decomposed into three components:  $f_0$  for dc,  $f_1$  for the first harmonic frequency of  $\omega$ , and  $f_2$  for the second harmonic  $2\omega$ . These components will be calculated as

$$\begin{aligned} f_0 &= \frac{1}{2} \frac{\partial c}{\partial x} (V_s^2 + \frac{1}{2} V_d^2), \\ f_1 &= \frac{\partial c}{\partial x} V_s v_d, \\ f_2 &= -\frac{1}{4} \frac{\partial c}{\partial x} V_d^2 \cos 2\omega t, \end{aligned} \tag{2}$$

where  $\partial c / \partial x$  is a partial differential of the capacitor,  $c$ , with respect to the displacement,  $x$ , and is assumed a constant.

Each component of the electrostatic force in Eq.(2) produces the steady-state displacement  $x$ , which also can be decomposed into  $x_0$ ,  $x_1$ , and  $x_2$  such as  $x_0 = |T_m(j0)|f_0$ ,  $x_1 = X_1 \sin(\omega t + \angle T_m(j\omega))$ , and  $x_2 = X_2 \cos(2\omega t + \angle T_m(j2\omega))$ , where  $X_1 = |T(j\omega)|(\partial c / \partial x) V_s V_d$  and  $X_2 = -(1/4)(\partial c / \partial x) |T(j2\omega)| V_d^2$ .

2.2 Electrical Model

The input charge  $q$  can be found as  $q = cv = [C_0 + (\partial c / \partial x)(x_0 + x_1 + x_2)](V_s + v_d)$  and its first harmonic component can be obtained approximately as  $q_1 = [C_0 + (\partial c / \partial x)x_0]v_d + (\partial c / \partial x)x_1 V_s$ . The first harmonic component of the input current  $i_1$  of a charge amplifier can be obtained by differentiating  $q_1$ . Therefore the admittance can be calculated as

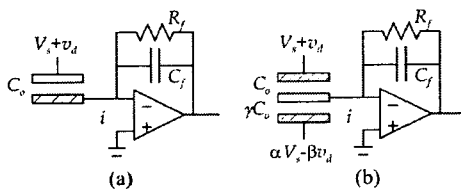


Fig. 1 Schematic diagram of (a) one-port actuator and (b) differential type actuator of which the capacitors are used both driving and sensing. Hatched plates represent stationary electrodes. The capacitor can be a parallel plate type or comb type.

$$Y(j\omega) = j\omega(C_0 + \frac{\partial C}{\partial x} x_0) + j\omega(\frac{\partial C}{\partial x} V_s)^2 T(j\omega) \quad (3)$$

The first term in Eq.(3) shows the electrical capacitors in the steady state and the second one shows the mechanical properties of the actuator. The zeros of the admittance in Eq.(3) are called parallel resonant frequencies or anti-resonant frequencies.

### 3. Differential Actuator

#### 3.1 Modeling

While the characteristics of one-port actuator in frequency domain are well understood, differential type actuator is not the case. Since it is driven differentially, the electrostatic force,  $f$ , has one component  $f_1$  assuming the symmetric or ideal condition that  $\alpha=1$ ,  $\beta=1$ , and  $\gamma=1$ , where  $\alpha$ ,  $\beta$ , and  $\gamma$  represent symmetry errors in biasing, driving, and capacitors, respectively (see Fig. 1(b)). In this case, the first harmonic input current can not flow into the charge amplifier. Therefore its admittance is zero and it has no characteristics in frequency domain.

In real case, however, there must be some errors in biasing or driving and also between capacitors. Because of these errors, the charge imbalance occurs and therefore the input current flows out from the common node of the differential type actuator. This current results in the admittance of the actuator.

Considering these errors, the electrostatic force can be decomposed into three components and found as

$$\begin{aligned} f_0 &= \frac{1}{2} \frac{\partial C}{\partial x} [(1-\alpha^2)V_s^2 + \frac{1}{2}(1-\beta^2)V_d^2], \\ f_1 &= \frac{\partial C}{\partial x} (1+\alpha\beta)V_s v_d, \text{ and} \\ f_2 &= -\frac{1}{4} \frac{\partial C}{\partial x} (1-\beta^2)V_d^2 \cos 2\omega t. \end{aligned} \quad (4)$$

Each component of the electrostatic force in Eq.(4) produces the steady-state displacement  $x$ , which can be decomposed into  $x_0$ ,  $x_1$ , and  $x_2$  such as  $x_0 = |T_m(j0)|f_0$ ,  $x_1 = X_1 \sin(\omega t + \angle T_m(j\omega))$ , and  $x_2 = X_2 \cos(2\omega t + \angle T_m(j2\omega))$ , where  $X_1 = |T(j\omega)|(\partial C/\partial x)(1+\alpha\beta)V_s V_d$ , and  $X_2 = -(1/4)(\partial C/\partial x)|T(j2\omega)|(1-\beta^2)V_d^2$ .

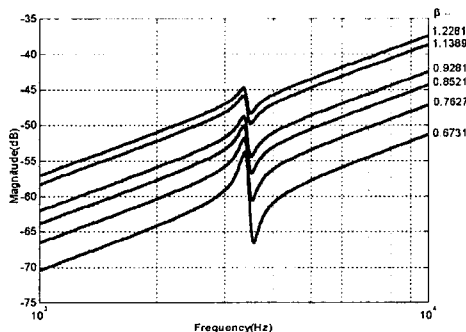


Fig. 2. Calculated waveform for the admittance of the differential actuator ( $\alpha=1.0032$  and  $\gamma=1.9954$ ).

Similarly the first harmonic component of the charge can be obtained approximately as

$$\begin{aligned} q_1 &= [(1-\beta\gamma)C_0 + \frac{\partial C}{\partial x}(1+\beta)x_0]v_d \\ &+ \frac{\partial C}{\partial x}(1-\alpha)x_1 V_s. \end{aligned} \quad (5)$$

Differentiating it, we can obtain the first harmonic component,  $i_1$ , of the input current of a charge amplifier. Therefore the admittance can be calculated as

$$\begin{aligned} Y(j\omega) &= j\omega[(1-\beta\gamma)C_0 + \frac{\partial C}{\partial x}(1+\beta)x_0] \\ &+ j\omega(\frac{\partial C}{\partial x} V_s)^2(1-\alpha)(1+\alpha\beta)T(j\omega). \end{aligned} \quad (6)$$

As shown in Eq.(6), in ideal case, the admittance will be zero since  $x_0=0$ .

In Eq.(6), it has a series resonant frequency and anti-resonant frequency like an one-port electrostatic actuator or a quartz crystal device. Using this approximated equation of Eq. (6), the admittance for the differential actuator is plotted in Fig. 2 with the same condition to the real case.

#### 3.2 Experimental Verification

Figure 3 shows how the admittance of the actuator are affected by the parameter  $\beta$ . The admittance curves are measured by varying the parameter  $\beta$  in the arithmetic unit (A.U.) in Fig. 4 while  $\alpha$  is set almost constant ( $\alpha \approx 1$ ). The capacitive sensor is used without injecting the modulating signal  $v_m$ .

The uncertain two parameters,  $\gamma$ , which represents the capacitive mismatch in the actuator including parasitic capacitors, the nominal capacitance,  $C_0$ , of the actuator of one side, are calculated as  $\gamma=1.9954$  and  $C_0 \approx 0.7pF$ , respectively, using the least square algorithm from the measured data at 10kHz. Experimental parameters are given in Table 1.

Compared with the calculated waveform of the admittance in Fig. 2, the measured waveform is well matched. Therefore the admittance model of the differential type actuator in Eq. (6) can be concluded to be effective.

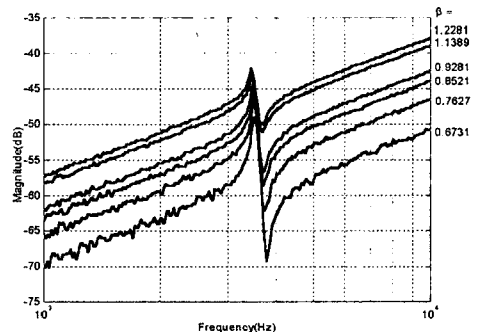


Fig. 3. Measured waveform for the admittance of the differential actuator.

### 3. Capacitive Sensor

By sensing the capacitance variation, a capacitive sensor detects displacement or its causes (force, pressure, acceleration, angular velocity, or so). Modulation and demodulation technique is used to obtain larger signal (change in capacitance) with less noise. The capacitive sensor used in this paper has a sample and hold device as a demodulator.

When two square-wave modulating signals  $v_{m1}$  and  $v_{m2}$  of the magnitude  $V_m$  ( $v_{m1} + v_{m2} = V_m$ ) are injected to the stators (see Fig. 1(b)), the first harmonic component,  $i_1$ , of the input current of the capacitive sensor will be given as

$$i_1 \approx \frac{\partial C}{\partial x} [(1-a)V_s + 2v_{m1} - V_m] \frac{dx_1}{dt} + [(1-\beta\gamma)C_0 + \frac{\partial C}{\partial x}(1+\beta)x_0] \frac{dv_d}{dt} + 2 \frac{\partial C}{\partial x} x_1 \frac{dv_{m1}}{dt} \quad (7)$$

Since we want to detect only the displacement  $x_1$ , the first and second terms are undesirable, which represent the admittance of the actuator (see Eq. (5)).

Figure 5 shows the admittance curve (dotted line) of the actuator and two frequency response curves measured by a capacitive sensor (solid line,  $V_o/V_d$ ) and LDV (laser doppler vibrometer, Polytec, OFV3001, OFV512) (dash-dotted line,  $X/V_d$ ) which are normalized by their dc gain.

In admittance curve, anti-resonant frequency is shown right after the resonant frequency, which results from some errors in biasing and driving or capacitive mismatch.

The frequency response curve measured by a capacitive sensor have two components as shown in Eq. (7). Above 7kHz, the admittance term is dominant in frequency response curve measured by the capacitive sensor. Because of this admittance term, the frequency response curve is distorted in comparison to the curve measured by LDV.

### 4. Discussion

The admittance model is derived assuming that the electrostatic actuator is comb-type and  $\partial C/\partial x$  is constant. But, the electrostatic actuator used in this

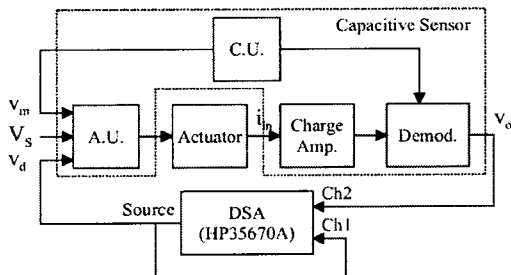


Fig. 4. Experimental setup. C.U., A.U., and DSA stand for control unit, arithmetic unit, and dynamic signal analyzer, respectively.

Table 1.

Experimental parameters

Parameter	Value	Parameter	Value
Bias voltage	12V	Rf	100kΩ
Driving voltage	2V	Cf	2pF
Mod. voltage	1V	Gain	10
Mod. freq.	120kHz	Sampling freq.	120kHz

paper does not have comb shape nor parallel plate but very complex shape to increase the force-generation capability. The small errors between the calculated and measured waveforms in Fig. 2 and Fig. 3 may be caused by these unsatisfied assumptions but the result, however, well agrees with the model. For the detailed description of the electrode shapes of the actuator, see [3].

### 5. Conclusion

The admittance of the differential-type electrostatic actuator is modeled and analyzed with a result that it is a function of biasing error, driving error, and capacitive mismatch including parasitic capacitors and therefore the anti-resonant frequency can be seen like one-port electrostatic actuator. However this admittance distorts the frequency response curve obtained by a capacitive sensor in high frequency range.

### Reference

- [1] M. W. Putty *et al*, "One-port active polysilicon resonant microstructures, " *IEEE MEMS '89*, pp. 60-65, 1989.
- [2] D. J. Ijntema *et al*, "Static and dynamic aspects of an air-gap capacitor, " *Sensors and Actuators, A*, Vol. 35, pp. 121-128, 1992.
- [3] S. Jung *et al*, "Optimal shape design of a rotary microactuator, " *IEEE J. of Microelectromechanical Systems*, Vol. 10, No. 3, pp. 460-468, 2001.

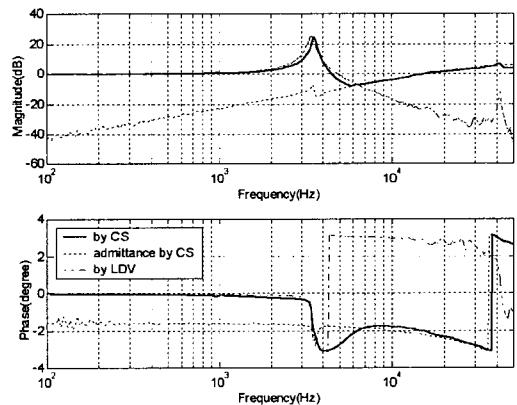


Fig. 5. Frequency response curves measured by a capacitive sensor(CS) and LDV.